COMPARISON OF LMI BASED $\mathcal{H}_2$ CONTROL DESIGNS FOR VSC-HVDC TRANSMISSION

Martyn Durrant * **Katarina Aleksic** **
Herbert Werner * **Keith Abbott** ***

* *Institute of Control Engineering, Hamburg University of Technology, Hamburg 21073 Germany*
** *Department for Automatic Control, University of Nis,18000 Nis, Serbia and Montenegro*
*** *Areva T&D Ltd, Power Electronic Systems, Stafford, England*

Abstract: The design of a robust controller for a VSC HVDC terminal using LMI based robust $\mathcal{H}_2$ and multi-objective $\mathcal{H}_2 - \mathcal{H}_\infty$ design methods is described. The operating range of the terminal is first characterised as an uncertainty region around a linear nominal model using the operating points of a non-linear model. The performance and robustness of controllers designed using the two methods and the effects of approximations in the uncertainty region definition are then described and compared. The best trade-off between robustness and performance on the non-linear model is demonstrated to be achieved using the robust $\mathcal{H}_2$ method.

Keywords: Power transmission, multi-variable feedback control, uncertain linear systems, robust stability, robust performance

1. INTRODUCTION

VSC HVDC transmission (Voltage Source Converter High Voltage Direct Current transmission) is an electrical transmission technology that has received considerable attention in recent years due to the development of high power transistor technology (Schettler *et al.*, 2000). A VSC HVDC transmission system connects two AC networks using two AC-DC terminals and a DC link. In such systems it is necessary to control power flow between the terminals under different AC network operating conditions, while at the same time controlling the terminal AC and DC voltages. This is a robust control problem which becomes increasingly challenging as the impedance of the network increases (Durrant *et al.*, 2003).

LMI based multi-objective output controller synthesis (Scherer, 1997) allows full-order controllers to be designed which optimise, with some conservatism, the $\mathcal{H}_2$ performance of a closed loop nominal operating point while ensuring stability all the plants in a set Ω_Δ around this point. Controllers with better nominal $\mathcal{H}_2$ performance are found by introducing a scaling matrix into the formulation and finding a local optimum solution iteratively using a method similar in concept to DK iteration. This method is referred to as 'Mixed Design' in this paper. The robust $\mathcal{H}_2$ design method referred to as KS iteration in (Farag, 2004) optimises the worst case $\mathcal{H}_2$ performance across Ω_Δ using a similar iterative scheme. In this paper this method is referred to as 'Robust $\mathcal{H}_2$ Design'.

This paper describes the application of these two methods to the problem of controlling power de-

livered and AC voltage at one terminal of a VSC HVDC transmission system. In this application stability during movement between operating points is an important requirement, as large load changes can occur virtually simultaneously following electrical faults. A potentially attractive feature of both design methods, that without this requirement would introduce unnecessary conservatism, is that the controllers designed are quadratically stable across Ω_Δ, so the controller can withstand arbitrarily fast changes in operating conditions within this set.

This paper first describes the non-linear analytical model of the terminal, the control objectives, and the generalised model used for design and the controller synthesis methods. Then the performance and robustness of controllers designed using these methods are presented and compared.

2. VSC HVDC MODEL

An 8th order non-linear model of a VSC-HVDC terminal attached to an AC network has been developed and successfully validated against a rigorous model including realistic converter behaviour (Durrant *et al.*, 2003). The model behaviour varies as a function of the reactance X_n (representing load) of the attached AC network and the power P delivered from it. The model inputs are the VSC control voltages v_{cld} and v_{clq}, the model outputs are P and the converter terminal voltage $|v_l|$. The physical units used in this paper are normalised (pu) units.

3. CONTROL OBJECTIVES

The power P and converter terminal voltage $|v_l|$ are to be controlled using inputs v_{cld} and v_{clq} with no steady state error between P and $|v_l|$ setpoints and measurements. The setpoint of $|v_l|$ is 1.0pu.

Closed loop stability is to be maintained at 52 power and network reactance operating points within the ranges $0 < P < 1.0$pu, $0.05 < X_n < 1.0$pu and while moving between them. The most important movements are step changes in power demand at constant values of X_n and step changes in X_n at constant power P.

A power response time of less than 0.15 s in response to a power setpoint step at a nominal operating point, and good damping and minimal variation of $|v_l|$ in response to power setpoint steps at all operating points are also required.

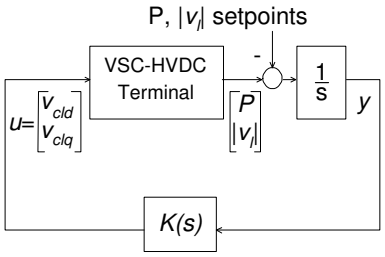

Fig. 1. Control loop structure

4. CONSTRUCTION OF A GENERALISED MODEL

To provide offset free tracking of P and $|v_l|$ setpoints in closed loop, the setpoint errors of the plant are passed through integrators, as shown in Figure 1.

The non-linear model is linearized at each of the operating points to explicitly allow consideration of operating point variation during controller synthesis. The set of models augmented by the output integrators, denoted $\mathcal{P}$, has members $p_i = \{A_i, B_i, C\}$ of 10th order whose C matrices are identical as a result of the output integrators.

$$\begin{aligned} \dot{x} &= A_i x + B_0 u, \qquad \forall p_i \in \mathcal{P} \\ y &= Cx \end{aligned} \tag{1}$$

The nominal plant matrices A_0 and B_0 are defined as the matrix of the A_i and B_i matrix element averages across the range of operating points. The variation in the B matrix is not included in the results presented in this paper, as including this variation was found to make little difference to the design. The operating points p_i are first represented by the deviations of the augmented plant matrices A_i from A_0, $A_{\delta i}$.

$$A_{\delta i} = A_i - A_0 \qquad \forall p_i \in \mathcal{P} \tag{2}$$

The A matrix variation is then represented by an uncertainty block Δ connected between fictitious output z_1 and input w_1 leading to the state space representation:

$$\begin{aligned} \dot{x} &= A_0 x + B_0 u + B_{w1} w_1 \\ y &= Cx \\ z_1 &= C_{z1} x \\ w_1 &= \Delta z_1 \end{aligned} \tag{3}$$

the A matrix of which depends on the value of Δ:

$$\dot{x} = (A_0 + B_{w1} \Delta C_{z1}) x + B_0 u \tag{4}$$

The singular value decomposition method of (Werner *et al.*, 2003) determines B_{w1} and C_{z1} of compatible dimensions such that they approximately cover, by projection, the variation of the operating points through the A matrix in $\mathcal{P}$:

$$A_{\delta i} \approx B_{w1} \Delta_i C_{z1}, \qquad ||\Delta_i|| < 1, \forall p_i \in \mathcal{P} \tag{5}$$

where the matrices in the set $\mathbf{\Delta}_u = \{\Delta_i(p_i) : p_i \in \mathcal{P}, \Delta_{2i} \in \mathbb{R}^{u\times u}\}$ are functions of the operating points p_i, and u is selected based on the accuracy of the approximation required. $\mathbf{\Delta}_u$ hence characterises the set of operating points. As detailed and explained in (Durrant *et al.*, 2004), application of this method demonstrates that the uncertainty set with $u = 2$, $\mathbf{\Delta}_2$, provides a reasonable characterisation of the operating range for this application. The further projection onto the set $\mathbf{\Delta}_{2d} = \{\Delta_{2di} = \delta_i I_2 : |\delta_i| < 1, \delta_i \in \mathbb{R}\}$ introduces little further error and enables structure to be taken advantage of in the design through the use of the scaling matrix $S \in \mathbb{R}^{2\times 2}$ introduced in Section 5.

The generalised model is completed by adding $\mathcal{H}_2$ performance input and output channels w_2 and z_2. The control loop is closed by $K(s)$.

$$\begin{aligned} sx &= A_0 x + B_0 u + B_{w1} w_1 + B_{w2} w_2 \\ z_1 &= C_{z1} x \\ z_2 &= C_{z2} x + D_{z2u} u \\ y &= Cx + D_{yw2} w_2 \\ u &= K(s) y \end{aligned} \tag{6}$$

The closed loop transfer functions from w_1 to z_1 and w_2 to z_2 and their associated state space representations are T_1, T_2 and $\{A_{cl}, B_{cl1}, C_{cl1}, D_{cl1}\}$, $\{A_{cl}, B_{cl2}, C_{cl2}, D_{cl2}\}$.

5. MIXED DESIGN

As a consequence of the small gain theorem, the system (6) with $w_1 = \Delta z_1$ is stable for all $||\Delta|| < \rho, \Delta \in \mathbf{\Delta}_{2d}$ if $\exists X_1 = X_1^T > 0, S = S^T > 0 \in \mathbb{R}^{2\times 2}$ such that: (Apkarian *et al.*, 1996):

$$\begin{bmatrix} A_{cl}^T X_1 + X_1 A_{cl} & X_1 B_{cl1} & C_{cl1} S \\ B_{cl1}^T X_1 & -S & D_{cl1}^T S \\ S C_{cl1}^T & S D_{cl1} & -\frac{1}{\rho^2} S \end{bmatrix} < 0 \tag{7}$$

The condition $||T_2||_2 < \nu$ is satisfied iff $\exists X_2 = X_2^T > 0, W = W^T$ such that:

$$\begin{bmatrix} A_{cl}^T X_2 + X_2 A_{cl} & X_2 B_{cl2} \\ B_{cl2}^T X_2 & -I \end{bmatrix} < 0$$

$$\begin{bmatrix} W & C_{cl2} \\ C_{cl2}^T & X_2 \end{bmatrix} > 0 \tag{8}$$

$$trace(W) < \nu^2$$

By setting $X_2 = X_1 = X$, fixing S and ρ and performing the transformation described in (Chilali and Gahinet, 1996) these inequalities become a set of LMIs in variables corresponding to the state space matrices of the full order controller $K(s)$ and the closed loop Lyapunov matrix X. By fixing the controller related matrices in the same inequality an alternative set of LMIs in X and S is formed. The iterative design method referred to in this paper as Mixed Design finds $K(s)$ that locally minimises ν over $K(s)$ and S; starting from $S = I_2$, ν is alternately minimised over these two sets of LMIs until there is little change in ν.

6. ROBUST $\mathcal{H}_2$ DESIGN

For the system (6) with $w_1 = \Delta z_1$ the cost J is defined as the maximum expected energy in z_2 over all uncertainties $\Delta \in \mathbf{\Delta}_{2d}$ with unit variance white noise stochastic inputs w_2 :

$$J = \max_{\mathbf{\Delta}_{2d}} E(||z_2(t)||_2^2) \tag{9}$$

$\sqrt{J}$ is the worst case value of the $\mathcal{H}_2$ norm between w_2 and z_2 over $\mathbf{\Delta}_{2d}$. J satisfies $J < trace(W)$ for all $||\Delta|| < \rho, \Delta \in \mathbf{\Delta}_{2d}$ if $\exists P = P^T > 0, W = W^T, S = S^T > 0 \in \mathbb{R}^{2\times 2}$ such that (Apkarian *et al.*, 1996):

$$\begin{bmatrix} X A_{cl}^T + A_{cl} X & X C_{cl2}^T & X C_{cl1}^T & \frac{1}{\rho} B_{cl1} S \\ C_{cl2} X & -I & 0 & 0 \\ C_{cl1} X & 0 & -S & 0 \\ \frac{1}{\rho} S B_{cl1}^T & 0 & 0 & -S \end{bmatrix} < 0$$

$$\begin{bmatrix} W & B_{cl2}^T \\ B_{cl2} & X \end{bmatrix} > 0 \tag{10}$$

As for Mixed Design, this inequality condition is transformed into a set of inequalities in variables corresponding to the matrices of the full order controller $K(s)$. Robust $\mathcal{H}_2$ Design is an analagous iterative scheme to the one described in Section 5: a $K(s)$ which locally minimises $trace(W)$ over $K(s)$ and S is found. $trace(W)$ is alternately minimised over LMIs in $K(s)$ related variables with S fixed, and LMIs in S with $K(s)$ related variables fixed.

7. RESULTS

In this section the results of applying the methods of section 5 ('Mixed Design') and 6 ('Robust $\mathcal{H}_2$ Design') to design controllers are described. The values of B_{w1} and C_{z1} corresponding to the uncertainty set $\mathbf{\Delta}_2$ described in Section 4 are used. Selecting either dimension of Δ greater than 2 leads to infeasibility in the LMIs.

The behaviour of the resulting closed loop systems are described in terms of nominal performance, robust stability and robust performance. The consequences of using an approximate uncertainty description in the design are also explained. Trade-offs between performance and robustness measures are then described and used to select the most appropriate controller for use on the nonlinear model.

The Matlab LMI toolbox (Gahinet *et al.*, 1995) was used to solve the LMIs. Gaps occur in graphs when either the LMIs are infeasible or closed loops are unstable.

7.1 Tuning Parameters

The $\mathcal{H}_2$ performance matrices in the design are chosen as:

$$B_{w2} = \begin{bmatrix} B_0 & 0 \end{bmatrix} \quad C_{z2} = \begin{bmatrix} qC \\ 0 \end{bmatrix}$$
$$D_{z2u} = \begin{bmatrix} 0 \\ I_2 \end{bmatrix} \quad D_{yw2} = \begin{bmatrix} 0 & 0.1I_2 \end{bmatrix} \tag{11}$$

The tuning parameters investigated in this paper are q, the penalty on the augmented plant output movement (that is, the integrated outputs of the true plant) and ρ, the fraction of the B_{w1} and C_{z1} defined uncertainty used in the design, as inspired by (Farag, 2004); ρ hence defines the size of Ω_Δ. q is used predominantly to adjust performance while ρ is used predominantly to adjust robustness. Setting $q < 0.3$ produces closed loop responses that are too slow for this application while $q > 1.0$ and $\rho > 0.25$ lead to infeasibility in the LMIs.

7.2 Notation Used In This Section

$\mu_{\Delta R}$ and $\mu_{\Delta C}$ are the real and complex structured singular values between w_i and z_i with respect to the structure $\mathbf{\Delta}_{2d}$. $\gamma_\Delta = 1/\rho^*$, where ρ^* is the largest value of ρ such that the LMI in (7) is satisfied, is the 'structured $\mathcal{H}_\infty$ norm' between w_i and z_i with respect to the structure $\mathbf{\Delta}_{2d}$.

$T_{2,\Delta}$ is the transfer function from w_2 to z_2 of system (6) with the performance weights in (11) with $q = 1$ and $w_1 = \Delta z_1$. $||T_2^*||_2 = \max_{\Delta \in \mathbf{\Delta}_2} ||T_{2,\Delta}||_2$; that is, the maximal $\mathcal{H}_2$ norm of the plants created by projecting the true plant uncertainties onto $\mathbf{\Delta}_2$. $\mathcal{P}_{H2}$ is the set of plants $\mathcal{P}$ augmented with $\mathcal{H}_2$ channels whose weights are as in (11) with $q = 1.0$. $||G_2^*||_2$ is the maximal $\mathcal{H}_2$ norm from w_2 to z_2 of the plants in $\mathcal{P}_{H2}$. R_{H2} is the ratio of $||G_2^*||_2$ to $||T_{2,0}||_2$, the nominal operating point $\mathcal{H}_2$ norm.

t_{90P} is the power rise time in response to a power setpoint change on the nominal plant. ζ_P^* is the damping factor of the dominant poles in the response of power to a step in power setpoint for the worst case operating point.

7.3 Nominal Performance as a Function of q

The graph in Figure 2 shows the effect of changing q and ρ on the nominal rise time of the power response. As anticipated, the rise time increases as q reduces and as ρ increases. The rise times for the Robust $\mathcal{H}_2$ Design are slightly higher than for the Mixed Design, as anticipated from the Robust $\mathcal{H}_2$ Design's minimisation of the worst case $\mathcal{H}_2$

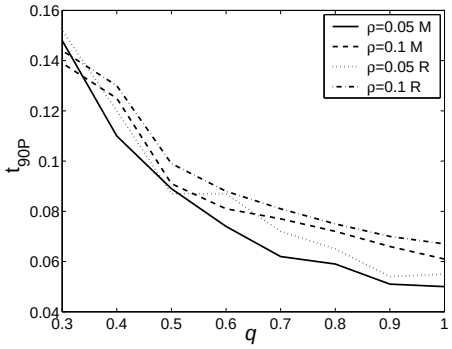

Fig. 2. t_{90P} as a function of q for indicated values of ρ:M= Mixed Design, R= Robust $\mathcal{H}_2$Design

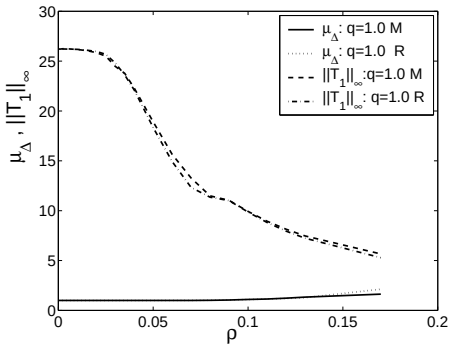

Fig. 3. $||T_1||_\infty$ and $\mu_{\Delta R}$: M= Mixed Design R= Robust $\mathcal{H}_2$ Design

norm over all the operating points in Ω_Δ rather than the nominal $\mathcal{H}_2$ norm. Other measures of nominal performance, including the nominal $\mathcal{H}_2$ norm, exhibit similar patterns of behaviour.

7.4 Robust Stability

The graph in Figure 3 shows $||T_1||_\infty$ and $\mu_{\Delta R}$ as functions of ρ for $q = 1.0$ for the two design methods. Very similar trends were found for $0.3 < q < 1.0$. The variations of the measures are similar for the two design methods suggesting, not unexpectedly, a similarity between them.

The reduction of $||T_1||_\infty$ with ρ indicates an increase in robustness against time variant uncertainties with ρ, as anticipated. $||T_1||_\infty$, γ_Δ and $\mu_{\Delta C}$ have almost identical values at each value of ρ, with $||T_1||_\infty > \gamma_\Delta > \mu_{\Delta C}$. The closeness of these measures indicates that the structure does not have a significant role in the robustness against the time-variant or dynamic, time invariant uncertainties that define γ_Δ and $\mu_{\Delta C}$ respectively. γ_Δ is of particular interest in this application as robustness against rapidly changing operating conditions is desirable. However it may be conservative, and unfortunately provides no guarantees in this application as it is always greater than 1.0. $1/\rho - \gamma_\Delta$ represents the conservatism in the design in terms of robust stability, and is only significant for $\rho < 0.04$.

$\mu_{\Delta R}$, which must be less than 1 for all the operating points to be stable, gradually increases with ρ from a minimum value of 0.98. It is counter-intuitive but not inconsistent for this application that while the other robustness measures improve with increasing ρ, $\mu_{\Delta R}$ deteriorates. The lower bound on $\mu_{\Delta R}$ is explained by the fact that with the uncertainty Δ between z_i and w_i set to the value $\Delta = -1.02I_2$ the system becomes open loop unstable.

7.5 Performance at True And Projected Operating Points

There is in the approach used a progression of projections from the true operating points to the operating points explicitly considered in the controller design. This starts with the projection of the 'true' uncertainty corresponding to the operating points onto the set $\mathbf{\Delta}_2$, continues with the further projection onto the structured set $\mathbf{\Delta}_{2d}$, and ends with use of the fraction of the operating region $\rho < 1.0$.

The graph on Figure 4 shows $\mathcal{H}_2$ norms corresponding to this progression for Robust $\mathcal{H}_2$ Design, for a range of values of ρ at $q = 1.0$: $||G_2^*||_2$, $||T_2^*||_2$, $||T_{2,-I_2}||_2$, and $||T_{2,-\rho I_2}||_2$. In each of these designs $-\rho$ is the most extreme operating point explicitly considered.

$||T_{2,-\rho I_2}||_2$ increases smoothly with ρ. However, the other three norms, particularly $||G_2^*||_2$, all exhibit fluctuation as ρ increases, suggesting that performance at the most extreme point considered in the design is not necessarily a good measure of performance, or even stability, at later stages in the progression of projections. These norms are also more sensitive to the values of the design parameters ρ and q than $||T_{2,-\rho I_2}||_2$ is. The physical explanation for this behaviour is that extreme operating points are very close to point where the open loop plant becomes unstable, leading to the $\mathcal{H}_2$ norm and other measures of closed loop performance becoming sensitive to the controller dynamics. This explains why clear trade-offs between robustness and performance are not found, as discussed further in Section 7.7.

7.6 Robust Performance

R_{H2} can be considered as a robust performance indicator, as it is a measure of deterioration of $\mathcal{H}_2$ performance from nominal to worst case. The graph of Figure 5 shows R_{H2} for the two design methods with $q = 1.0$ and $q = 0.3$; for low values of ρ, R_{H2} reduces with ρ for Robust $\mathcal{H}_2$ Design as anticipated, but increases for Mixed Design before reducing. Robust $\mathcal{H}_2$ Design is marginally better

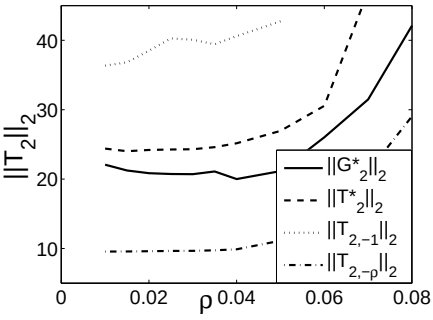

Fig. 4. $\mathcal{H}_2$ for progression from true operating points to design: Robust $\mathcal{H}_2$ Design, $q = 1.0$

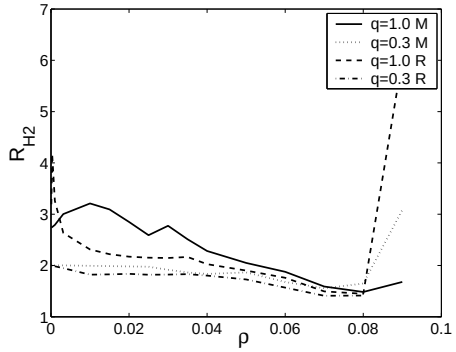

Fig. 5. R_{H2} for Mixed and Robust $\mathcal{H}_2$ design

in this respect than Mixed design. At $\rho > 0.08$ there is a sharp increase in R_{H2} that correlates with a sharp increase in $||T_{2,-\rho I}||_2$.

As q is increased there is more deterioration in the $\mathcal{H}_2$ norm between nominal and worst case performance although nominal performance improves.

7.7 Trade off between performance and robustness

A natural trade-off between performance and robustness to consider for the design methods used is the one between $||T_{2,0}||_2$ and R_{H2} - it is expected that a low value of R_{H2} may only be achieved at the expense of a large value of $||T_{2,0}||_2$. However, performance and robustness measures that are more aligned to the control objectives for this application are t_{90P} and $1/\zeta_P^*$, good damping (a low value of $1/\zeta_P^*$) only being expected to be achieved at the expense of a relatively long rise time. The graph on Figure 6 plots $1/\zeta_P^*$ against t_{90P} for controllers designed using the 2 methods with $0.3 < q < 1.0$ and $0 < \rho < 0.25$. The trade-off is not distinct because of the sensitivity of $||T_2||_2$ and ζ_P^* to design parameters as explained in Section 7.5, and because these trade-off parameters are not explicitly considered in the design. The Robust $\mathcal{H}_2$ Designs are on average closer to the best trade offs. The controller which minimises $1/\zeta^*$ for $t_{90P} < 0.15s$ is a Robust $\mathcal{H}_2$ Design with $\rho = 0.08$ and $q = 0.3$. This is close to the point where R_{H2} is minimised for this value

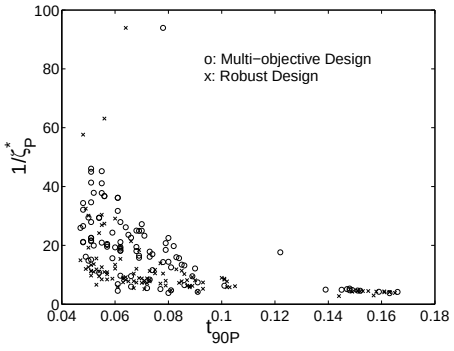

Fig. 6. ζ_P^* against t_{90P}

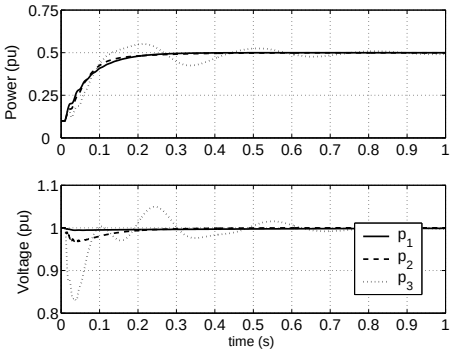

Fig. 7. Non-linear model step response

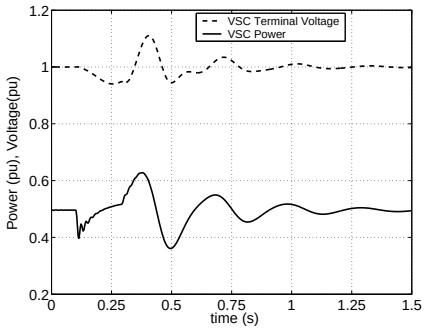

Fig. 8. Response to change in network reactance

of q. Figure 7 shows the nonlinear model power and voltage responses to power setpoint changes of 0.4pu with this controller at operating points p_1 (X_n = 0.05pu), p_2 (X_n = 0.25pu) and p_3 (X_n = 1.0pu). The response to a step change in X_n from 0.05pu to 1.0pu is shown in Figure 8. These responses demonstrate that the control objectives are successfully fulfilled. Robust performance against such large changes in operating point is not guaranteed by the robust analysis measures of Section 7.4; however in practice large values of ζ_P^* and low values of R_{H2} are found to be good indicators of performance for the non-linear plant in this application.

8. CONCLUSIONS

Controllers for VSC-HVDC have been successfully designed which achieve robust stability and good robust performance at each of a range of non-linear operating conditions using LMI based $\mathcal{H}_2$ techniques. $\mathcal{H}_2$ weights and the fraction of the operating region considered by the design were used as tuning parameters.

The distinctions between Robust $\mathcal{H}_2$ and Mixed designs are not large in this application and are made less clear by the unpredictable nature of robust performance measures at extreme operating points. The Robust $\mathcal{H}_2$ design gave marginally better results overall.

$\mathcal{H}_2$ methods that include full block multipliers are likely to lead to lower conservatism than the designs described here, allowing a better trade-off between nominal and robust performance. These approaches are a subject for further research.

9. ACKNOWLEDGEMENTS

The support of Areva T&D for this work is acknowledged.

REFERENCES

Apkarian, P., G. Becker, P. Gahinet and H. Kajiwara (1996). *LMI techniques in Control Engineering: from Theory to Practice*. SIAM.

Chilali, M. and P. Gahinet (1996). H_∞-design with pole placement constraints: An LMI approach. *IEEE Trans. Automatic Control* **41**(3), 358–367.

Durrant, M., H. Werner and K. Abbott (2003). Model of a VSC HVDC terminal attached to a weak AC system. *IEEE CCA 2003 Proceedings*.

Durrant, M., H. Werner and K. Abbott (2004). Synthesis of multi-objective controllers for a VSC HVDC terminal using LMIs. *IEEE CDC 2004 Proceedings*.

Farag, A O (2004). A Practical Approach to Control Design Using Linear Matrix Inequalities. PhD thesis. TUHH Hamburg.

Gahinet, P., A. Nemirovski, A. Laub and M. Chilali (1995). *LMI Control Toolbox*. The Mathworks Inc.

Scherer, C. (1997). Multi-objective Output-Feedback Control Via LMI Optimisation. *IEEE Transactions on Automatic Control* **42**(7), 896–911.

Schettler, F., H. Huang and N. Christl (2000). HVDC transmission using voltage sourced converters - Design and Applications. *IEEE summer power meeting 2000, Seattle*.

Werner, H., P.Korba and Tai-Chen-Yang (2003). Robust tuning of power system stabilizers using LMI-techniques. *IEEE Transactions on Control Systems Technology* **11**, 147–52.